NeuroImage: Clinical 28 (2020) 102416

Contents lists available at ScienceDirect

NeuroImage: Clinical

journal homepage: www.elsevier.com/locate/ynicl

Reproducible metabolic topographies associated with multiple system atrophy: Network and regional analyses in Chinese and American patient cohorts

Bo Shen[a,1], Sidi Wei[a,1], Jingjie Ge[b], Shichun Peng[d], Fengtao Liu[a], Ling Li[b], Sisi Guo[c], Ping Wu[b], Chuantao Zuo[b], David Eidelberg[d], Jian Wang[a,2,*], Yilong Ma[d,2,*]

[a] Department of Neurology and Institute of Neurology, Huashan Hospital, Shanghai Medical College, Fudan University, Shanghai, China
[b] PET Center, Huashan Hospital, Fudan University, Shanghai, China
[c] Department of Neurology, Shuguang Hospital, Shanghai University of Traditional Chinese Medicine, Shanghai, China
[d] Center for Neurosciences, Institute of Molecular Medicine, The Feinstein Institutes for Medical Research, Northwell Health, Manhasset, NY, USA

ARTICLE INFO

Keywords:
Multiple system atrophy
Metabolic brain network
Differential diagnosis of parkinsonism
Functional brain mapping
PET

ABSTRACT

Purpose: Multiple system atrophy (MSA) is an atypical parkinsonian syndrome and often difficult to discriminate clinically from progressive supranuclear palsy (PSP) and Parkinson's disease (PD) in early stages. Although a characteristic metabolic brain network has been reported for MSA, it is unknown whether this network can provide a clinically useful biomarker in different centers. This study was aimed to identify and cross-validate MSA-related brain network and assess its ability for differential diagnosis and clinical correlations in Chinese and American patient cohorts.

Methods: We included ^{18}F-FDG PET scans retrospectively from 128 clinically diagnosed parkinsonian patients (34 MSA, 34 PSP and 60 PD) and 40 normal subjects in China and in the USA. Using PET images from 20 moderate-stage MSA patients of parkinsonian subtype and 20 normal subjects in both centers, we reproduced MSA-related pattern (MSAPRP) of spatial covariance and estimated its reliability. MSAPRP scores were evaluated in assessing differential diagnosis among moderate- and early-stage MSA, PSP or PD patients and clinical correlations with disease severity. Regional metabolic differences were detected using statistical parameter mapping analysis. MSA-related network and regional topographies of metabolic abnormality were cross-validated between the Chinese and American cohorts.

Results: We generated a highly reliable MSAPRP characterized by decreased loading in inferior frontal cortex, striatum and cerebellum, and increased loading in sensorimotor, parietal and occipital cortices. MSAPRP scores discriminated between normal, MSA, PSP and PD subjects and correlated with standardized ratings of clinical stages and motor symptoms in MSA. High similarities in MSAPRPs, network scores and corresponding maps of metabolic abnormality were observed between two different cohorts.

Conclusion: We have demonstrated reproducible metabolic topographies associated with MSA at both network and regional levels in two independent patient cohorts. Moreover, MSAPRP scores are sensitive for evaluating disease discrimination and clinical correlates. This study supports differential diagnosis of MSA regardless of different patient populations, PET scanners and imaging protocols.

1. Introduction

Multiple system atrophy (MSA) is a rare, fatal neurodegenerative disorder characterized by symptoms of autonomic failure plus parkinsonism, cerebellar ataxia, or both. It is still challenging to distinguish MSA from idiopathic Parkinson's disease (PD) and progressive supranuclear palsy (PSP) with well-established clinical diagnostic criteria (Hughes et al., 2002; Obelieniene et al., 2018), especially in early

* Corresponding authors at: Department of Neurology, Huashan Hospital, Fudan University, 12th Wulumuqi Zhong Road, Shanghai 200040, China. Center for Neurosciences, the Feinstein Institutes for Medical Research, 350 Community Drive, Manhasset, New York 11030, USA. (Y. Ma).
E-mail addresses: wangjian_hs@fudan.edu.cn (J. Wang), yma@northwell.edu (Y. Ma).
[1] Contributed equally to this work.
[2] Contributed equally to this work.

https://doi.org/10.1016/j.nicl.2020.102416
Received 29 February 2020; Received in revised form 29 August 2020; Accepted 3 September 2020
Available online 09 September 2020

Table 1
Demographic and clinical characteristics of normal controls and moderate-stage parkinsonian patients in the USA and China.

	N	Gender (M/F)	Age (years)	HY Scale	UPDRS (motor)	Duration (years)
Combined moderate-stage cohort						
Normal Control	20	7/13	62.3 ± 8.8	N/A	N/A	N/A
MSA	20	10/10	61.7 ± 7.4	3.9 ± 0.9*	46.8 ± 14.5*	3.3 ± 2.4*
PSP	20	12/8	65.5 ± 8.4	3.9 ± 0.7*	35.0 ± 12.4	3.1 ± 1.7†
PD	40	26/14	61.0 ± 5.2	2.7 ± 1.3	31.3 ± 18.3	6.8 ± 4.6
Moderate-stage American cohort						
Normal Control	10	3/7	64.3 ± 7.6	N/A	N/A	N/A
MSA	10	3/7	63.7 ± 8.7	4.6 ± 0.5‡	43.4 ± 17.1	3.5 ± 2.2
PSP	10	5/5	68.1 ± 5.8	3.4 ± 0.9	26.2 ± 14.9‡	2.5 ± 1.2
PD	20	14/6	60.1 ± 5.4	3.1 ± 1.5	29.7 ± 18.8	9.3 ± 4.5§
Moderate-stage Chinese cohort						
Normal Control	10	4/6	60.2 ± 9.9	N/A	N/A	N/A
MSA	10	7/3	59.7 ± 5.7	3.6 ± 0.8	49.6 ± 11.9	3.2 ± 2.8
PSP	10	7/3	62.8 ± 10.0	4.1 ± 0.6	39.5 ± 8.5	3.6 ± 2.0
PD	20	12/8	61.9 ± 5.1	2.5 ± 1.1	32.6 ± 18.3	4.8 ± 3.8

Data are given as mean ± standard deviation. MSA: multiple system atrophy; PSP: progressive supranuclear palsy;
PD: Parkinson's disease; HY: Hoehn and Yahr; UPDRS: unified Parkinson's disease rating scale. Modified from our previous study (Ge et al., 2018).
* $P < 0.005$ compared to the PD group in the combined cohort (*post-hoc* Bonferroni tests).
† $P < 0.001$
‡ $P < 0.05$ compared to the corresponding group in the Chinese cohort (two-sample *t* tests).
§ $P < 0.005$

diagnosis (Rizzo et al., 2016). Given the great differences in pathogenesis, treatment response and prognosis among MSA, PSP and PD, the accuracy of differential diagnosis and rigorous evaluation are very important for both clinical and research applications.

Major clinical phenotypes of parkinsonism are neuropathologically defined entities: MSA and PD belong to synucleinopathies with accumulation of α-synuclein aggregates in oligodendrocytes and neurons respectively (Tong et al., 2010), while PSP and corticobasal syndrome (CBS) are tauopathies with the core pathophysiology of tau fibrillar aggregates (Boxer et al., 2017). Since parkinsonian disorders also involve the degeneration of dopaminergic neurons in the substantia nigra, dopaminergic imaging can reveal abnormal nigrostriatal innervation with several PET (Van Laere et al., 2010; Oh et al., 2012; Kaasinen et al., 2019) and SPECT (Cummings et al., 2011; Tatsch and Poepperl, 2013; Kraemmer et al., 2014) radioligands. However, whether this approach can differentiate atypical parkinsonism specifically from PD is currently not yet confirmed (Stoessl et al., 2014; Ko et al., 2017).

Despite the clinical heterogeneity of disease manifestations, metabolic activity assessed with ^{18}F-fluorodeoxyglucose (^{18}F-FDG) PET in conjunction with multivariate computing algorithms has revealed disease-specific brain network patterns in parkinsonism (Ma et al., 2007; Eckert et al., 2008; Teune et al., 2013; Matthews et al., 2018). It can reliably differentiate between various parkinsonian syndromes even during early stages (Spetsieris et al., 2009; Tang et al., 2010; Tripathi et al., 2016) by measuring expression scores of multiple disease patterns prospectively in any new subjects. Of note, we have previously cross-validated metabolic network patterns related with PD and PSP respectively in Chinese populations against their American counterparts (Wu et al., 2013; Ge et al., 2018). Although MSA-related pattern (MSAPRP) had been defined independently in American and European patients with predominantly parkinsonian subtype of MSA (MSA-P) (Eckert et al., 2008; Teune et al., 2013), and was found to be similarly expressed in American and Korea patients with both subtype of MSA-P and subtype of MSA with cerebellar ataxia (MSA-C) (Poston et al., 2012; Ko et al., 2017), this potential network marker for MSA has not yet been vigorously cross-validated in multiple patient cohorts on different scanners.

In this study we pursued these goals: (1) used multivariate brain network analysis to identify MSAPRP in combined Chinese and American patients with MSA-P and normal subjects; (2) evaluated network scores in assessing differential diagnosis in moderate- and early-stage patients with parkinsonism as well as clinical correlations with disease severity; (3) conducted cross-validation to identify MSAPRP in the American or Chinese cohort separately and measure its activity in the other cohort; (4) localized brain regions with metabolic abnormality in the same images and probed similarities/differences across the two cohorts using univariate brain mapping analysis; (5) examined the reproducibility of MSA-specific network and regional metabolic characteristics across study populations, PET instruments and analytic approaches.

2. Material and methods

2.1. Subjects

The vast majority of parkinsonian and normal (NL) subjects described in this article had been used in the previous report focusing solely on the identification and validation of PSP-related metabolic patterns (Ge et al., 2018). To identify and cross-validate MSAPRP between different clinical centers, we retrospectivly selected two independent cohorts of moderate-stage parkinsonian and NL subjects from the USA and China in this study (n = 100). The American cohort included 50 participants: 10 MSA-P, 10 PSP and 20 PD patients along with 10 matched NL controls enrolled at North Shore University Hospital (NY, USA). To match the sample size the Chinese cohort was comprised of the same numbers of subjects: 10 MSA-P, 10 PSP, 20 PD, and 10 NL subjects recruited at the Department of Neurology of Huashan Hospital (Shanghai, China). All patients were rated clinically for symptom severity by Hoehn and Yahr (HY) scale and the unified Parkinson's disease rating scale (UPDRS). All subject groups underwent ^{18}F-FDG PET at the respective study sites, and were highly similar in their clinical and demographic information (Table 1). In the combined American and Chinese cohort, age was matched across four subject groups ($F[3,96] = 1.8$, $P = 0.15$; ANOVA). However, MSA/PSP patients were more advanced in terms of clinical HY stages ($P < 0.005$; *post-hoc* Bonferroni tests) and motor ratings ($P < 0.005$) but had shorter disease duration ($P < 0.005$) than PD patients, suggesting consistent motor symptoms among all patient groups. The American cohort had more advanced clinical HY stages in MSA ($P < 0.05$, two-sample *t*-test, two-tailed), lower motor ratings in PSP ($P < 0.05$) and longer duration in PD patients ($P < 0.005$) compared to their Chinese counterparts.

To further verify the value of MSAPRP in early differential diagnosis we enrolled another independent Chinese cohort (n = 68) with early-

Table 2
Demographic and clinical characteristics of normal controls and early-stage parkinsonian patients in China.

	N	Gender (M/F)	Age (years)	HY Scale	UPDRS (motor)	Duration (years)
Early-stage Chinese Cohort						
Normal Control	20	12/8	56.9 ± 11.5	N/A	N/A	N/A
MSA	14	8/6	52.1 ± 7.2*	2.6 ± 0.9§	33.3 ± 12.8‡	1.4 ± 0.5
PSP	14	9/5	65.6 ± 8.2§	3.2 ± 1.1§	29.6 ± 20.0	1.5 ± 0.6
PD	20	14/6	50.9 ± 11.3*	1.5 ± 0.7	16.2 ± 7.9†	1.1 ± 0.5

Data are given as mean ± standard deviation. MSA: multiple system atrophy; PSP: progressive supranuclear palsy;
PD: Parkinson's disease; Hoehn and Yahr; UPDRS: unified Parkinson's disease rating scale. Modified from our previous study (Ge et al., 2018).
* $P < 0.005$ compared to the PSP group (*post-hoc* Bonferroni tests).
† $P < 0.05$
‡ $P < 0.005$ compared to the PD group (*post-hoc* Bonferroni tests).
§ $P < 0.001$

stage parkinsonian disorders: 14 MSA, 14 PSP and 20 PD patients along with 20 matched NL controls (Table 2). These patients were initially scanned with ^{18}F-FDG PET at the Chinese site as clinically uncertain cases and then followed up for several years until a clinical diagnosis was made by their neurologists. MSA patients were presented with parkinsonism and signs of autonomic symptoms within the first 2y from disease onset; all MSA-P subtypes except one case diagnosed as MSA-C after 2y of follow-up, given predominant cerebellar ataxia manifesting progressively. Comparing this cohort to the combined cohort, MSA/PD subjects were younger ($P < 0.001$) with PSP ($P = 0.95$) and NL subjects ($P = 0.11$) closely matched in age; the patients had lower motor ratings (MSA: $P < 0.001$; PSP: $P = 0.39$; PD: $P < 0.0001$; two-sample *t*-tests, two-tailed) and shorter disease duration ($P < 0.005$).

The clinical diagnosis was unknown to the investigators involved in imaging studies with the neurologists blinded to imaging outcomes during clinical follow-up. Two senior specialists of movement disorders followed all parkinsonian patients at each site for at least one year. A probable diagnosis of MSA based on the consensus criteria (Gilman et al., 2008) requires a sporadic, progressive adult-onset disorder including rigorously defined autonomic failure and poorly levodopa-responsive parkinsonism or cerebellar ataxia. The non-motor symptoms typically include lost smell, constipation, incontinence, orthostatic hypotension and impotence, and comorbidities such as sleep behavior disorder and depression (See data for all Chinese patients with MSA in Supplementary Table 1). PSP and PD patients were screened based on the NINDS-SPSP (Respondek et al., 2013) and the UK Brain Bank diagnostic criteria (Hughes et al., 1992) respectively. Any parkinsonian patients suspected of having other neurological diseases such as vascular parkinsonism had been ruled out by brain MRI scans during routine clinical examination at both sites. All normal controls in this study had no history of neurologic or psychiatric disorders without prior exposure to neuroleptic agents or drug use. While the American patients had moderate-stage parkinsonism as diagnosed clinically (Tang et al., 2010), the vast majority of the Chinese patients at both early and moderate stages had neurodegenerative parkinsonism as confirmed retrospectively by differential reduction in striatal dopamine transporters with PET (Insert Supplementary Fig. 1 here).

2.2. ^{18}F-FDG PET imaging and processing

All subjects were asked to fast for at least 6 h but had free access to water, and antiparkinsonian medications in patients were withheld for at least 12 h before PET imaging. The USA site used a GE Advance tomograph (Milwaukee, WI). A PET transmission scan was first performed for attenuation correction with a 10-min emission scan acquired in 3D mode between 35 and 45 min after intravenous bolus injection of ^{18}F-FDG (~185 MBq). The Chinese site used a Siemens Biograph 64 PET/CT (Munich, Germany). Following a short CT scan, a 10-min PET scan was started 45-min post-injection. Only relative glucose metabolic activity was measured as no arterial blood sampling was taken in this clinical imaging protocol. All studies in patients and NL controls were performed in a resting state in a quiet and dimly lit room.

Images were processed by Statistical Parametric Mapping (*SPM5*) software (Wellcome Department of Imaging Neurosciences, Institute of Neurology, London, UK) implemented in Matlab 7.4.0 (Mathworks Inc, Sherborn, MA). All scans were spatially normalized into a standard brain space and smoothened by a Gaussian filter of 10-mm FWHM over a 3D space to increase the signal to noise ratio for statistical analysis.

2.3. Network analysis of metabolic activity

Metabolic brain network analysis was conducted using a voxel-based spatial covariance mapping algorithm termed SSM/PCA (Spetsieris et al., 2009), implemented in *ScanVp* software freely available online (http://www.feinsteinneuroscience.org at Center for Neuroscience, the Feinstein Institutes for Medical Research, Manhasset, NY). Briefly, by extracting covariance data in brain images after removing mean effects across voxels and subjects, group-wise PET data (following natural log-transform) are reduced to a series of independent covariance maps and corresponding subject scores. A disease-specific metabolic pattern is defined by linearly combining a set of orthogonal principal components (PCs) whose expression maximally discriminates the patient and NL groups by logistic regression and whose topography represents a spatially distributed network of functionally interrelated, covarying brain regions. This covariance brain network depicts the degree of regional covariation often described as loading on a voxel basis. Here MSAPRP was first identified using ^{18}F-FDG PET data from moderate MSA-P and NL subjects in the combined American and Chinese cohort. The reliability of MSAPRP was estimated at each voxel with a bootstrapping scheme (Habeck et al., 2008). Network scores of MSAPRP were computed for all subjects (NL, MSA, PSP or PD) using a voxel-based topographic profile rating algorithm (Ma et al., 2007; Peng et al., 2014), by averaging the product of each image with the network pattern over the brain.

To verify the consistency of MSAPRP between different centers we next identified a separate MSAPRP using ^{18}F-FDG PET scans of moderate MSA-P and NL subjects in the American or Chinese cohort. Inter-cohort cross-validation utilized two quantitative indicators of topographic distribution and network expression. Regional loadings were correlated between the two patterns among significant voxels (absolute values ≥ 1.0) in the whole brain. Network scores of MSAPRP in the American cohort were calculated for the subjects from China and compared with those from the USA or vice versa. Network scores in MSA and NL groups from the USA or China were also compared across the two MSAPRPs. All network scores were Z-scored using subject scores of the NL controls included in the identification of each MSAPRP.

2.4. Regional analysis of metabolic activity

Differences in regional metabolic activity between patients and

controls were detected at each voxel according to the general linear model in *SPM* software as we described (Ge et al., 2018). For the American or Chinese cohort (together or separately), we performed a two-sample *t*-test to characterize metabolic activity in moderate MSA compared with controls. ANCOVA was used to model inter-subject differences in global metabolic activity over the whole brain. We also utilized a flexible factorial design to compare regional metabolic activity between the American and Chinese cohorts using *SPM* software (Ge et al., 2018). The site and group were two main effects with global values included as a covariate to remove the potential confound. The regions with similar or different metabolic abnormality between the American and Chinese MSA patients versus respective controls were separately detected using conjunction or interaction analysis.

Significant brain regions were localized anatomically according to our previous study (Ge et al., 2018). We set a height threshold at $P < 0.001$ (uncorrected) over whole brain and searched for clusters that also survived at family-wide error (FWE)-corrected $P < 0.05$. The *SPM* maps for increased or decreased metabolic activity were overlaid on a standard T1-weighted MRI brain template in stereotaxic space. To quantify metabolic changes in specific regions *post-hoc*, we constructed a 4-mm radius spherical volume of interest within the image space, centered at the peak voxel of significant clusters in the SPM analysis. Globally normalized metabolic values were then calculated in patients and healthy controls with *ScanVP* software.

2.5. Statistical analysis

Differences in MSAPRP scores or regional metabolic values over multiple subject groups were assessed using one-way analysis of variance (ANOVA), with *post-hoc* contrasts examined by Bonferroni tests. Discrimination of MSAPRP scores among parkinsonian patients at different stages and NL subjects was determined by receiver operating characteristic (ROC) analysis. Relationships between MSAPRP scores and UPDRS motor ratings/disease duration, or between MSAPRP scores with-subject across two MSAPRPs were evaluated by Pearson correlations with non-parametric Spearman correlation for clinical HY stages. All analyses relied on SPSS software (SPSS Inc., Chicago, IL) and reported as significant at $P < 0.05$.

3. Results

3.1. MSA-related brain network pattern in the combined cohort

Spatial covariance analysis of ^{18}F-FDG PET scans in moderate MSA-P and NL subjects from the USA and China evaluated the first 6 PCs including 56.6% of subject × voxel variance. MSAPRP was selected from a linear combination of PC1, PC2, PC3, PC4, and PC6 (24.9% variance accounted for [VAF]) whose expression separated the groups maximally in the logistic regression model. This pattern was characterized bilaterally by reduced loading in inferior frontal cortices, striatum and posterior cerebellum, associated with increased loading in precentral/postcentral gyrus, and parietal/occipital cortices (Fig. 1A) and reliable according to bootstrapping with 1000 iterations ($P < 0.001$; Insert Supplementary Fig. 2A here). Subject scores of MSAPRP measured in this combined cohort of moderate parkinsonian patients showed a group effect (ANOVA: $F[3,96] = 133.1$, $P < 0.0001$; Fig. 1B) with elevation in MSA/PSP ($P < 0.0001$, *post-hoc* Bonferroni tests) but not in PD ($P = 1.0$) compared to NL groups. MSAPRP scores in PSP were also higher ($P < 0.0001$) than in PD but lower ($P < 0.0005$) than in MSA. These scores exhibited increased accuracy in discriminating MSA from PSP/PD/NL (area under the curve [AUC] = 0.82 ~ 1.00) or PSP from PD/NL (AUC = 0.99 ~ 1.00) according to the ROC analysis (Supplementary Table 2). Furthermore, MSAPRP scores did not differ between the two cohorts in NL, MSA, PSP and PD groups ($P \geq 0.083$, two-sample *t*-tests, two-tailed).

MSAPRP scores also showed a group effect in the Chinese cohort of early-stage patients (ANOVA: $F[3,64] = 23.3$, $P < 0.0001$; Fig. 1C) with elevation in MSA/PSP ($P < 0.0001$, *post-hoc* Bonferroni tests) but not in PD ($P = 1.0$) versus NL groups. These scores in MSA and PSP groups were similar ($P = 0.85$) although both were higher ($P < 0.0001$) than in the PD group. Likewise, MSAPRP scores disclosed increasing accuracy for discriminating MSA from PD/NL (AUC = 0.91) or PSP from PD/NL (AUC = 0.93) in this early-stage patient cohort (Supplementary Table 3). To realistically assess clinical correlates of parkinsonism, patients were combined in early- and moderate-stage cohorts. MSAPRP scores correlated with clinical HY stages (Spearman test: $r = 0.38$, $P = 0.04$; Fig. 2A) and UPDRS motor ratings (Pearson correlation: $r = 0.44$, $P = 0.012$; Fig. 2B) in the MSA group but not in the PSP/PD groups ($r \leq 0.07$, $P \geq 0.22$). No correlations with disease duration were present in any of patient groups.

3.2. Cross-validation of network patterns between the American and Chinese cohorts

The separate analysis of moderate MSA-P and NL subjects in the American or Chinese cohort probed the first 4 PCs with 53.9% or 54.4% of subject × voxel variance. MSAPRP for each cohort was selected from a linear combination of PC1 + PC2 + PC4 (28.3% VAF) or PC1 + PC4 (28.6% VAF) respectively. Both MSAPRPs revealed highly similar topographies (Fig. 3A/4A; c.f., Fig. 1A) which had strong voxel-based correlations between regional loadings in the brain ($r = 0.849$, $P < 0.0001$) and were also reliable according to bootstrapping with 1000 iterations ($P < 0.01$; Insert Supplementary Fig. 2B-C here). Subject scores of both MSAPRPs for the four relevant groups are provided in Table 4. ANOVA revealed effects of group across the American derivation cohort and the Chinese validation cohort ($F[3,36] = 72.9$, $P < 0.0001$; Fig. 3B) or vice versa ($F[3,36] = 60.2$, $P < 0.0001$; Fig. 4B). Subject scores of either MSAPRP were elevated ($P < 0.0001$, *post-hoc* Bonferroni tests) in MSA versus NL groups in both cohorts. These scores in the two MSA groups were similar ($P = 0.22$) for the American MSAPRP but differed ($P = 0.0001$) for the Chinese MSAPRP. These scores correlated across both groups for the identification of American MSAPRP and the validation of Chinese MSAPRP (Fig. 3C: $r = 0.867$, $P < 0.0001$; MSA: $r = 0.637$, $P < 0.05$; controls: $r = 0.256$, $P = 0.475$) or vice versa (Fig. 4C: $r = 0.954$, $P < 0.0001$; MSA: $r = 0.685$, $P < 0.05$; controls: $r = 0.421$, $P = 0.225$).

3.3. Differences in regional metabolic activity between MSA patients and normal controls

SPM analysis of ^{18}F-FDG PET scans from the USA and China revealed bilaterally distributed metabolic abnormality associated with moderate MSA-P compared to NL subjects (c.f., Insert Supplementary Fig. 3 here; Insert Supplementary Tables 4-6 here). In the combined data, relative metabolic activity decreased in middle/inferior frontal gyri, striatum, claustrum and cerebellum, but increased in medial/middle frontal, postcentral, inferior occiptial and superior/inferior temporal gyri as well as precuneus and uncus ($P < 0.001$; most survived at FWE-corrected $P < 0.05$). Regional metabolic differences between moderate MSA and normal subjects were similar in the American or Chinese cohort.

3.4. Similarities/differences in regional metabolic activity between the American and Chinese cohorts

Conjunction analysis localized many bilaterally overlapping brain regions of metabolic abnormality between the American and Chinese cohorts. Comparing moderate MSA-P with NL subjects, metabolic activity decreased in inferior frontal gyrus, striatum, claustrum and cerebellum, but increased in superior frontal/cingulate, postcentral and superior/middle temporal gyri, and hippocampus or parahippocampus (Fig. 5A, Table 3; $P < 0.001$, with some regions survived at FWE-

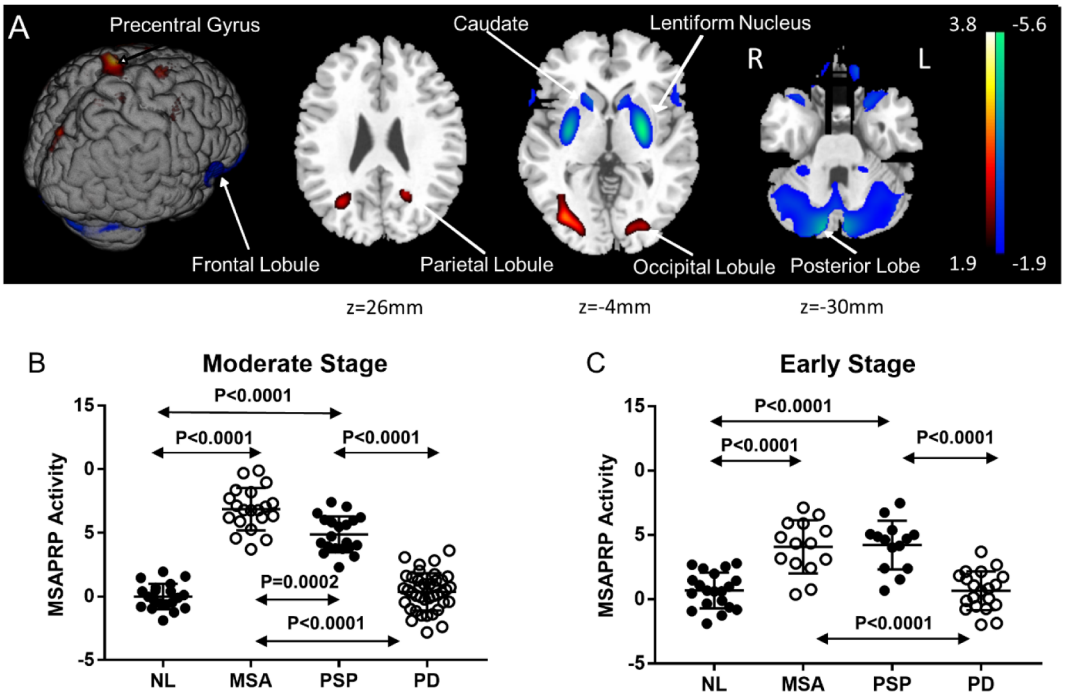

Fig. 1. MSAPRP identified by spatial covariance analysis of ^{18}F-FDG PET scans from moderate-stage MSA patients and normal (NL) controls in the combined American and Chinese cohort alongside MSAPRP expression for differential diagnosis. (A) Abnormal metabolic covariance topography in MSAPRP showing decreased/negative (*blue*) and increased/positive (*red*) regional loadings coded by *Z*-scored values. (B) MSAPRP activity discriminated MSA from NL subjects in the derivation sample (the two columns on the left) and from PSP or PD groups in the combined American and Chinese cohort at moderate stages. (C) MSAPRP activity distinguished MSA from NL and PD subjects in the Chinese cohort at early stages. The error bars denote standard deviations. MSA: multiple system atrophy; PSP: progressive supranuclear palsy; PD: Parkinson's disease; MSAPRP: MSA parkinsonian-related pattern; L/R: left and right sides of the brain. (For interpretation of the references to colour in this figure legend, the reader is referred to the web version of this article.)

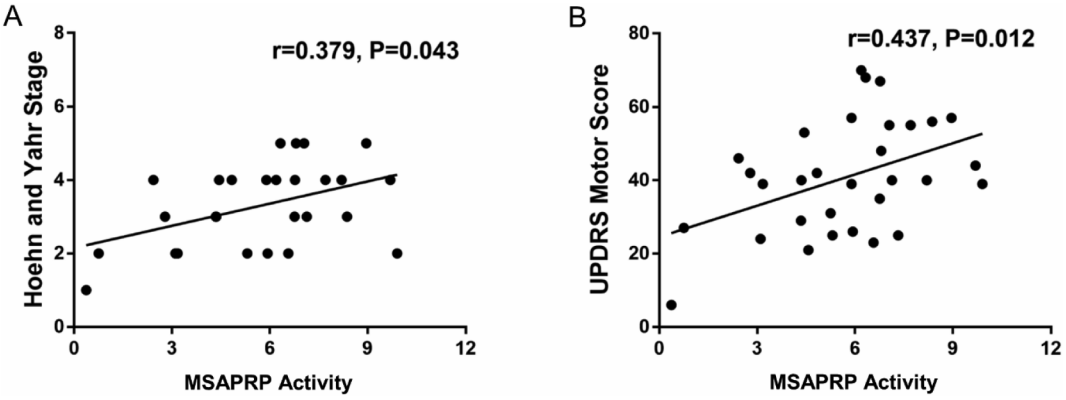

Fig. 2. MSAPRP expression for clinical correlations. MSAPRP activity correlated with clinical indicators of Hoehn and Yahr stages (A) and the Unified Parkinson's Disease Rating Scale (UPDRS) motor ratings (B) in the combined early- and moderate-stage MSA patients in China and moderate-stage MSA patients in the USA. MSA: multiple system atrophy; MSAPRP: MSA parkinsonian-related pattern.

corrected $P < 0.05$). Metabolic activity measured *post-hoc* in many primary regions showed group effects (Table 4) and decreases in striatum, claustrum, and cerebellum along with increases in superior frontal/postcentral/middle temporal gyri in MSA versus NL subjects across both cohorts (Fig. 5B-G; $P < 0.05$, *post-hoc* tests). Interaction analysis revealed positive MSA-related metabolic changes in precentral and middle occipital gyri, superior parietal lobule and cerebellum in the American versus the Chinese cohort (Supplementary Fig. 4; Supplementary Table 7; $P < 0.001$, none survived at FWE-corrected $P < 0.05$). The *post-hoc* analysis disclosed group effects (Table 4) with increased metabolism in middle occipital gyrus and superior parietal lobule in the American cohort but no changes in the Chinese cohort comparing moderate MSA-P to NL subjects, with less decreased cerebellar metabolism in the American cohort than in the Chinese cohort.

4. Discussion

We examined the characteristics and consistency of abnormal metabolic topographies in two independent cohorts of moderate MSA-P and normal subjects using multivariate and univariate analytic methods. These techniques are geared toward identifying unique brain networks with spatial covariance data or mapping differences in regional metabolic activity voxel-by-voxel using ^{18}F-FDG PET images in patients and normal controls (Ge et al., 2018; Habeck et al., 2008). Network analysis generally recovers more disease-specific, widely distributed brain regions that may not have direct biological correlates, whereas regional analysis is closer to the diagnostic process based on visual reading of clinical images. These two complementary approaches focus on covariance brain network or regional metabolic differences

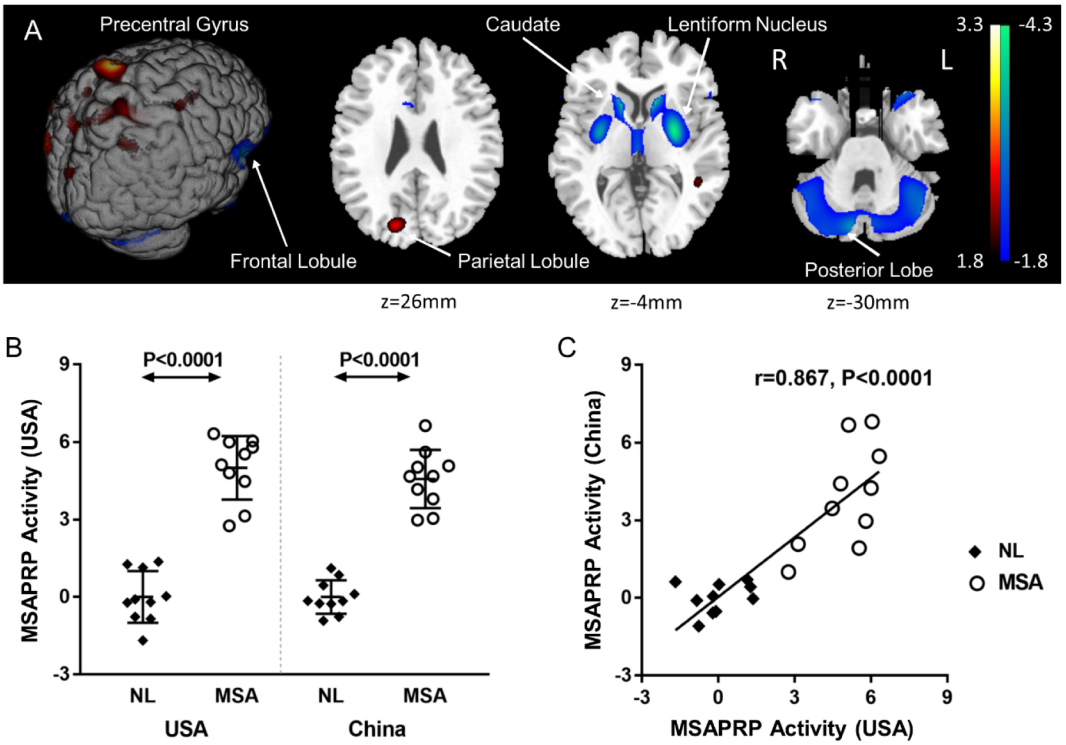

Fig. 3. MSAPRP identified by spatial covariance analysis of ^{18}F-FDG PET scans from moderate-stage MSA patients and normal (NL) controls in the American cohort. (A) Abnormal metabolic covariance topography in MSAPRP showing decreased/negative (*blue*) and increased/positive (*red*) regional loadings coded by *Z*-scored values. (B) MSAPRP activity discriminated moderate-stage MSA from NL groups in both the American and Chinese cohorts. The error bars denote standard deviations. (C) Individual scores in the American cohort correlated highly across both NL subjects and MSA patients used for the identification of MSAPRP in the USA and the validation of MSAPRP in China. MSA: multiple system atrophy; MSAPRP: MSA parkinsonian-related pattern; L/R: left and right sides of the brain. (For interpretation of the references to colour in this figure legend, the reader is referred to the web version of this article.)

and provide quantitative means for delineating pathophysiological changes in MSA at the systemic and local levels respectively.

This study included moderate-stage American and Chinese patient cohorts and early-stage Chinese patient cohort with consistent demographic and clinical characteristics, compatible with patient populations typically seen in clinical practice. We defined the covariance topography of MSAPRP in the combined American and Chinese sample and characterized the diagnostic performance and clinical correlations with network scores computed prospectively in multiple patient cohorts. Comparing the American and Chinese cohorts, MSAPRP

Table 3
Overlapping brain regions with significant metabolic differences in moderate-stage MSA patients versus normal controls across the American and Chinese cohorts.

Structure	Brodmann Area (BA)	Hemisphere	MNI Coordinates*			Zmax	Cluster Size (mm^3)
			X	Y	Z		
Decreased Metabolism †							
Inferior Frontal Gyrus	BA 45	L	−56	18	6	4.25	5000
Inferior Frontal Gyrus ‡	BA 45	R	60	16	0	5.31	6376
Lentiform Nucleus ‡		L	−28	−10	2	6.58	62,288
Caudate		L	−14	8	12	3.84	6312
Lentiform Nucleus		R	18	0	16	3.55	1208
Caudate		R	16	16	4	3.76	
Claustrum ‡		R	34	−8	−2	6.35	7720
Cerebellar Tonsil ‡		R	2	−54	−50	6.65	73,552
Increased Metabolism †							
Superior Frontal Gyrus	BA 6	L	–22	16	68	3.86	1120
Superior Frontal Gyrus ‡	BA 6	R	22	−16	70	6.28	253,496
Postcentral Gyrus ‡	BA 3	L	−28	−38	54	6.21	
Postcentral Gyrus ‡	BA 4	R	16	−40	66	6.21	
Cingulate Gyrus	BA 24	L	−14	−4	52	4.19	1384
Cingulate Gyrus	BA 24	R	20	6	52	4.53	1008
Superior Temporal Gyrus	BA 39	R	50	−54	6	4.67	4136
Middle Temporal Gyrus	BA 21	R	56	–32	−12	3.80	816
Middle Temporal Gyrus	BA 21	R	36	2	–32	3.68	1000
Hippocampus/Parahippocampus		L	−26	−10	−30	3.95	4632

* Montreal Neurological Institute (MNI) standard space.
† Survived at uncorrected $P < 0.001$, extent threshold = 100 voxels (800 mm^3).
‡ Survived at FWE $P < 0.05$. MSA: multiple system atrophy.

Table 4
Differences in brain network activity and regional metabolic values in moderate-stage MSA patients compared with normal controls across the American and Chinese cohorts.

	American Cohort		Chinese Cohort		F value ‡
	Normal Controls	MSASubjects	Normal Controls	MSA Subjects	
Network Analysis (SSM/PCA)					
MSAPRP Activity (USA)	**0.00 ± 1.00**	**4.99 ± 1.22**	0.00 ± 0.65	4.57 ± 1.13	72.9
MSAPRP Activity (China)	0.00 ± 0.59	3.91 ± 1.99†	**0.00 ± 1.00**	**7.22 ± 1.65**	60.2
Conjunction Analysis (SPM)					
Decreased Metabolism					
Inferior Frontal Gyrus (60 16 0)	46.3 ± 5.2	41.9 ± 4.7†	41.9 ± 4.5	34.2 ± 4.7	10.9
Lentiform Nucleus (-28–10 2)	81.5 ± 4.8	70.2 ± 8.2	85.2 ± 4.1	71.5 ± 8.2	12.5
Caudate (-14 8 12)	66.3 ± 5.7	56.9 ± 12.9	69.7 ± 13.7	53.8 ± 10.7	4.5
Claustrum (34–8 −2)	91.3 ± 3.4	78.6 ± 7.9	88.0 ± 5.5	75.3 ± 5.4	17.3
Cerebellar Tonsil (2–54 −50)	83.0 ± 5.5	73.7 ± 7.0†	86.5 ± 5.1	62.5 ± 5.3	34.7
Increased Metabolism					
Superior Frontal Gyrus (–22 16 68)	65.0 ± 4.0	69.7 ± 3.8†	66.6 ± 8.0	75.9 ± 5.1	7.7
Postcentral Gyrus (16–40 66)	80.1 ± 4.3*	87.9 ± 4.5†	84.0 ± 3.3	96.0 ± 6.2	21.1
Cingulate Gyrus (20 6 52)	79.4 ± 4.9	79.8 ± 2.8†	81.7 ± 2.7	87.7 ± 6.2	7.7
Middle Temporal Gyrus (36 2–32)	57.4 ± 2.2*	61.2 ± 3.2†	52.0 ± 4.4	55.0 ± 4.4	11.3
Interaction Analysis (SPM)					
Precentral Gyrus (-52–2 48)	86.9 ± 2.8*	90.4 ± 6.0†	94.0 ± 3.9	96.3 ± 5.6	7.5
Middle Occipital Gyrus (-26–94 12)	83.4 ± 3.6*	89.3 ± 4.5	90.5 ± 2.5	88.6 ± 7.2	4.3
Cerebellar Tonsil (0–56 −44)	85.1 ± 5.9*	76.3 ± 7.6†	90.6 ± 5.6	64.8 ± 5.6	32.8

Subject scores and regional metabolic values are presented as mean ± standard deviation. MSAPRP activity values marked bold indicated subject scores in the original derivation cohort with the other values computed prospectively in the validation cohort. MSA: multiple system atrophy; MSAPRP: MSA parkinsonian-related pattern.

* $P < 0.05$ compared to the normal group in the Chinese cohort (*post-hoc* Bonferroni tests).

† $P < 0.05$ compared to the MSA group in the Chinese cohort (*post-hoc* Bonferroni tests).

‡ $P < 0.05$ comparison among four independent groups in both cohorts (one-way ANOVA).

scores were in agreement for each of the moderate-stage parkinsonian subgroups coinciding with their similar clinical features. In both early- and moderate-stage patient cohorts, MSAPRP scores were elevated differently in MSA/PSP but not in PD (greater in MSA but similar in PSP/PD). These scores were independent of age but higher in woman than men in PD despite minor gender mismatch in normal controls. Of

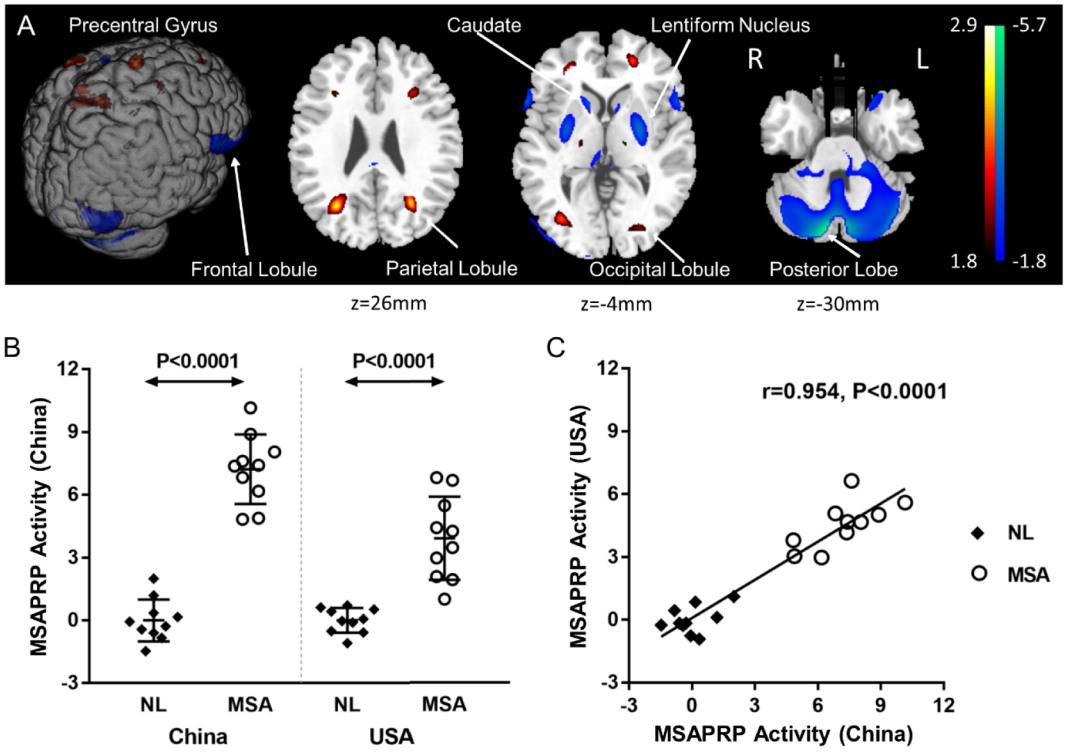

Fig. 4. MSAPRP identified by spatial covariance analysis of ^{18}F-FDG PET scans from moderate-stage MSA patients and normal (NL) controls in the Chinese cohort. (A) Abnormal metabolic covariance topography in MSAPRP showing decreased/negative (*blue*) and increased/positive (*red*) region loadings coded by *Z*-values. (B) MSAPRP activity discriminated moderate-stage MSA from NL groups in both the Chinese and American cohorts. The error bars denote standard deviations. (C) Individual scores in the Chinese cohort correlated highly across both NL subjects and MSA patients used for the identification of MSAPRP in China and the validation of MSAPRP in the USA. MSA: multiple system atrophy; MSAPRP: MSA parkinsonian–related pattern; L/R: left and right sides of the brain. (For interpretation of the references to colour in this figure legend, the reader is referred to the web version of this article.)

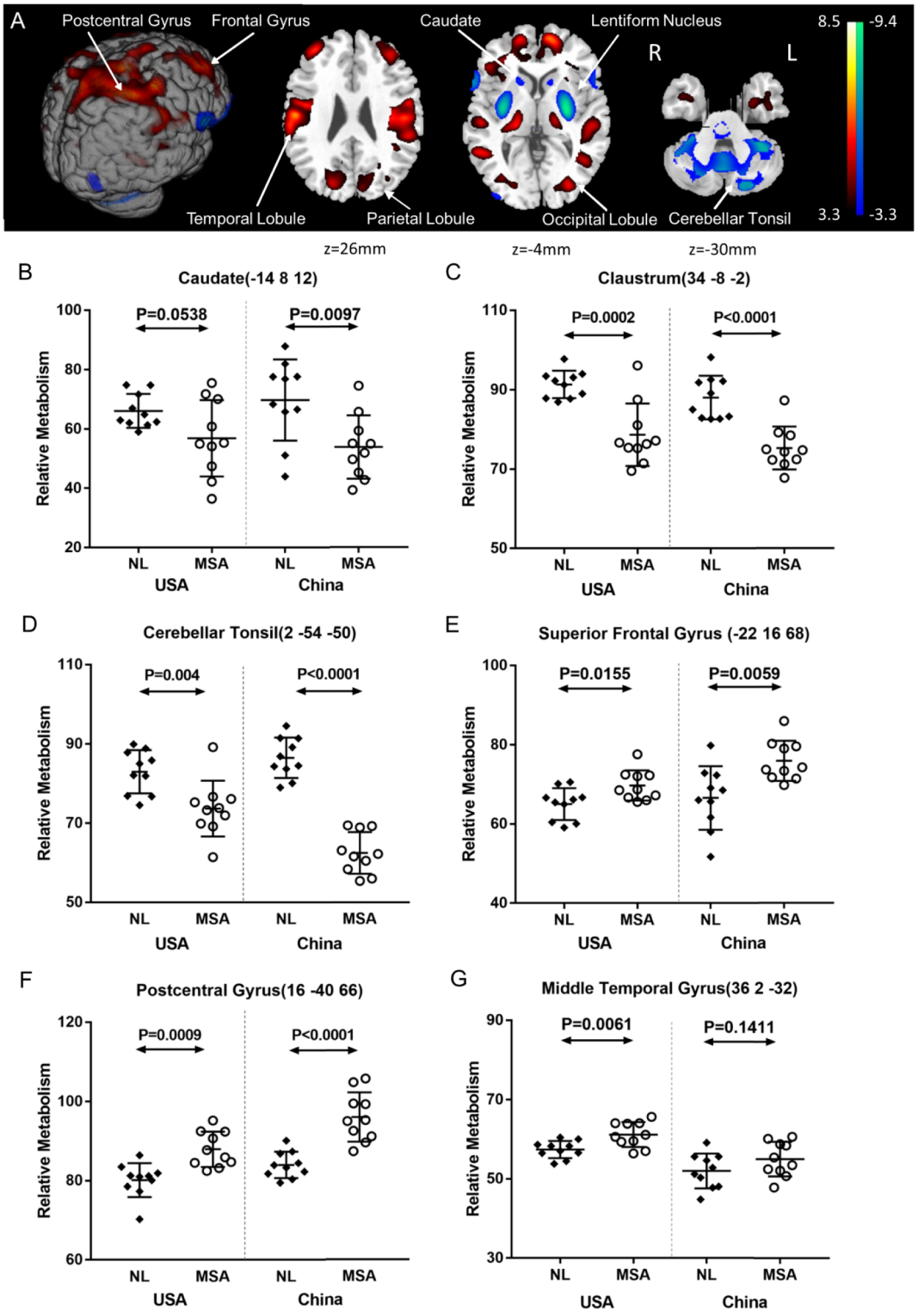

Fig. 5. Brain regions with similar metabolic abnormality in moderate-stage MSA patients compared to normal (NL) controls detected by conjunction analysis of ^{18}F-FDG PET scans with SPM across the American and Chinese cohorts. (A) Abnormal metabolic distribution of commonality (*T*-statistic maps) between the American and Chinese MSA patients showing decreased *blue*) and decreased (*red*) relative metabolic activity represented by *T*-statistic values ($P < 0.001$). (B-G) Group differences in relative metabolic values in select cortical and subcortical regions (4 mm-radius spheres) centered at the peak coordinates of significant clusters in the prior SPM analysis on a voxel-by-voxel basis. The error bars denote standard deviations. MSA: multiple system atrophy; SPM: statistical parametric mapping; L/R: left and right sides of the brain. (For interpretation of the references to colour in this figure legend, the reader is referred to the web version of this article.)

note, MSAPRP scores provided high accuracy to distinguish MSA from normal/PD but not from PSP subjects in the early- or moderate-stage parkinsonian cohort (Fig. 1B-C; Supplementary Table 2-3). Moreover, MSAPRP scores correlated positively with clinical HY stages and UPDRS motor ratings (Fig. 2A-B) in MSA after combining early- and moderate-stage patients. By contrast, no clinical association was seen in PSP or PD suggesting that unique features captured in MSAPRP do not manifest prominently in other forms of parkinsonism. The discrimination of MSA

from normal/PD subjects by MSAPRP scores and network correlation with clinical disability in MSA are both in line with prior reports in independent American and Korean patients (Poston et al., 2012; Ko et al., 2017) demonstrating their specificity and utility for gauging the symptomatology of MSA. Therefore, network scores of MSAPRP are cross-validated for use as a quantitative marker of disease severity.

This work revealed MSA-related topographical similarities in moderate MSA-P patients at network and regional levels in both American and Chinese cohorts when analyzed together or individually. The MSAPRP topography is characterized bilaterally by negative/decreased loading in inferior frontal gyrus, striatum and cerebellum with concurrent positive/increased loading in sensorimotor, parietal and occipital cortices. This was generally consistent with the original study depicting only negative/decreased striatal/cerebellar loading (Eckert et al., 2008) and the subsequent report of both negative and positive loadings in subcortical and cortical regions (Teune et al., 2013). Differences in the magnitudes of loading in MSAPRP suggested concomitant regional metabolic abnormality underlyng the progression of disease. The widespread cortical metabolic changes described in different studies may be secondary to striatal and cerebellar dysfunction. It is worth noting that cerebellar metabolic activity also decreased markedly even in the analysis involving only MSA patients of parkinsonian-type. We suspect that the rapid disynaptic pathway from the cerebellar dentate nucleus to the striatum may provide a pathophysiological basis for the simultaneous metabolic reduction in both cerebellum and striatum in MSA-P (Chen et al., 2014; Caligiore et al., 2017).

The patterns of regional metabolic abnormality associated with moderate MSA-P detected in this study mostly resembled topographies of corresponding MSAPRPs in the combined or separate American and Chinese cohorts (Insert Supplementary Fig. 3 here). Indeed, relative to normal controls, relative metabolic activity in moderate MSA-P patients decreased in inferior frontal gyrus, striatum and cerebellem, and increased in sensorimotor, parietal, temporal and occipital cortices as reported before (Eckert et al., 2005; Teune et al., 2010). These regions of reduced metabolic activity were also seen in patients with mixed MSA subtypes (Lyoo et al., 2008) and lower putamen/claustrum metabolic activity also coincided with perfusion SPECT data (Van Laere et al., 2004). Such relative metabolic decreases reflected largely brain atrophy in these regions underlying this disorder (Nemmi et al., 2019; Yang et al., 2019). Of note, some of the regions with increased metabolic values also extended to medial superior frontal gyrus and thalamus decribed previously (Eckert et al., 2005), which along with the temporal gyrus were also evident in MSAPRP at a lower threshold (reliabity $P < 0.01$). Such concordance can explain the elevated MSAPRP activity in MSA (Fig. 1B/3B/4B) since subject scores reflect similarity between individual metabolic images and the identified brain network. Accordingly, the elevated MSAPRP activity in PSP reported here and in Korean patients (Ko et al., 2017) also results from some overlap in metabolic abnormality (e.g., frontal, temporal and occipital cortices) between PSP and MSA (Eckert et al., 2005; Teune et al., 2010). Thus, both network and regional analysis methods can effectively identify MSA to a great extent given the inherent connection between system and local metabolic characteristics.

Some differences in MSA-related metabolic characteristics across two moderate-stage patient cohorts also existed in this study. Although we saw very strong topographic correlation of MSAPRPs in the USA and China ($R^2 = 0.72$) its magnitude was smaller than those (0.84 ~ 0.86) found previously for PDRP and PSPRP (Wu et al., 2013; Ge et al., 2018). That accounted for ~ 72% of total variance but still left ~ 28% variance unaccounted for. Of note, the MSAPRP from China has higher occipital loading than that from the USA, which contributed to lower reliability in such a relatively large region in the MSAPRP from the combined American and Chinese sample (see Fig. 1A; Supplementary Fig. 2A). To further explore residual differences in regional loading between the US and Chinese patterns we analyzed randomly selected bootstrap samples (n = 100 per pattern). This analysis revealed moderate correlations overall ($R^2 = 0.56 \pm 0.17$ [mean ± SD]; range = 0.39 ~ 0.73) using the same common mask defined from the two patterns by thresholding at $|\text{loading}| \geq 1.0$ (Supplementary Fig. 5A). The correlations were still robust between the US and Chinese patterns ($R^2 = 0.67$) with a magnitude of 0.48 ± 0.18 from the same set of bootstrap samples using the common mask defined by thresholding at $|\text{loading}| \geq 0.75$ (Supplementary Fig. 5B). In addition, comparing the US pattern to its Chinese counterpart, regional loading increased bilaterally in middle to superior occipital/temporal and post-central regions as well as in left inferior and precentral gyri at a lower threshold (Z-value = 2.0, $P < 0.025$, one-tailed; see Supplementary Fig. 5C). Of interest these regions were found to be located in less prominent territories in the original US and Chinese patterns with absolute loading values smaller than 0.75. These issues need to be further examined with large multi-center imaging data. Subject scores of both MSAPRPs were comparable in MSA of the American but not of the Chinese group. Nevertheless, these scores correlated moderately in MSA patients but not in normal subjects for whom MSAPRP was not supposed to be expressed. Moreover, we observed increased occipital metabolic activity in MSA in the US only with greater cerebellar decline in China (Table 4). Like the heterogeneity of MSA-related metabolic abnormality reported in prior studies these discrepancies could be contributed to differences in patient samples, imaging protocols and instrumentation (e.g., scanners, attenuation correction methods and image reconstruction algorithms).

Population-dependent genetic heterogeneity may also impact on the variation of metabolic network expression between the American and Chinese cohorts (Schindlbeck and Eidelberg, 2018; Wu et al., 2013; Ge et al., 2018). Although a genome-wide association study failed to reveal any genetic correlates of MSA due to small samples and high rates of misdiagnosis (Federoff et al., 2016), candidate pathogenic genes of MSA such as SNCA and COQ2 were reported to differ among human races in different geographic regions (Stamelou and Bhatia, 2016). Nonetheless, this cross-validation study in two independent cohorts proved that the disease-related metabolic characteristics were highly reproducible in major cerebral regions of MSA on a whole-brain basis (c.f., Fig. 1A/3A/4A), strongly supporting the notion that MSAPRP expression is well-qualified to be a reliable imaging marker in clinical diagnosis of MSA.

Although MSA cannot be accurately discriminated from PSP by MSAPRP scores in the early-stage cohort they could be separated by subject scores of PSP-related pattern as we reported (Ge et al., 2018). It would be of interest to determine whether diagnosis between these two atypical forms of parkinsonism could be enhanced by combining corresponding subject scores and relative metabolic values in brain regions defined by *SPM* analyses. This underscores the urgent need to improve early differenential diagnosis by joint discrimination with multiple-disease specific patterns (Tang et al., 2010; Tripathi et al., 2016) and multi-tracer or dual-phase molecular imaging techniques (Südmeyer et al., 2011; Jin et al., 2017). This study concludes the cross-validation of three metabolic patterns across the Chinese and American parkinsonian patient populations and paves the way for testing single-case differential diagnosis prospectively with the use of multiple disease-related patterns in China.

Several limitations are present in this study: (1) The diagnostic accuracy of parkinsonism relied on clinical expertise at each center without neuropathological confirmation. Nonetheless, the majority of the patients enrolled in China had been confirmed by reduced striatal dopaminergic function. (2) The sample sizes of MSA and normal subjects were relatively small at each site to keep with the MSAPRP originally established in the USA. These limited samples might be justifiable given the more severe metabolic abnormality inherent in this rapidly degenerative disease. This issue was mostly overcome by combining all PET images from the two sites in a series of primary analysis reported in this article. The fact that analogous metabolic patterns were identified across two independent cohorts suggests that the clinical diagnosis was reliable, and the sample sizes were adequate

in this study. (3) Image normalization for the analysis were done with *SPM5* and its default brain perfusion PET template to be compatible with our previous work (Wu et al., 2013; Ge et al., 2018). Before pursuing differential diagnosis based on network scores there is a need to migrate these disease-related patterns using newer versions of *SPM* and standardized high-resolution brain templates to keep pace with the progress of the field although no differences are anticipated between *SPM5* and *SPM8* according to the network study in PD (Peng et al., 2014). (4) This work focused on MSA-P but ignored the issue of MSA clinical subtypes as only one patient in the early-stage cohort had primary clinical features of MSA-C at follow-up but similar elevation in MSAPRP activity as in MSA-P as reported (Poston et al., 2012; Ko et al., 2017). More specific metabolic patterns may help better differentiate patients with MSA-P and MSA-C or other potential MSA subtypes such as pure autonomic failure in the future (Low et al., 2015). This is a topic worth further investigations.

5. Conclusion

This study revealed similar topographies in spatial covariance brain network and distribution of regional metabolic abnormality in subtype of MSA-P by combining ^{18}F-FDG PET images of moderate-stage patients and normal subjects from American and Chinese medical centers. Cross-validation between the two datasets confirmed highly reproducible MSA-related metabolic brain networks and regional activity patterns of cortical and subcortical abnormality across different patient populations and imaging instrumentation/protocols. MSA-related brain network was reliable on a voxel basis and its expression in individual subjects discriminated early to moderate MSA from normal controls or PD and correlated with clinical variables of disease stage and severity. Network score from ^{18}F-FDG PET may serve as an objective biomarker of MSA in patient care and clinical trials. Metabolic brain network in a large cohort of pathologically-confirmed patients and normal subjects from a single site or multiple centers can further establish the robustness of MSAPRP.

6. Compliance with Ethical Standards

Ethical approval

All procedures performed in studies involving human participants were in accordance with the ethical standards of the Institutional Review Boards at North Shore University Hospital (Manhasset, USA) and Huashan Hospital (Shanghai, China) and with the 1964 Helsinki declaration and its later amendments or comparable ethical standards. The study in the USA was also performed in compliance with the Health Insurance Portability and Accountability Act.

Informed consent

Written consent was obtained at each site from each subject following detailed explanation of the study procedures.

CRediT authorship contribution statement

Bo Shen: Validation, Writing - original draft, Writing - review & editing. **Sidi Wei:** Resources, Data curation, Visualization, Writing - original draft. **Jingjie Ge:** Methodology, Formal analysis, Investigation, Project administration. **Shichun Peng:** Methodology, Data curation, Formal analysis, Investigation, Software. **Fengtao Liu:** Resources, Data curation, Writing - original draft. **Ling Li:** Formal analysis, Investigation, Validation, Writing - review & editing. **Sisi Guo:** Resources, Data curation, Validation, Writing - original draft. **Ping Wu:** Resources, Data curation, Visualization, Formal analysis, Investigation. **Chuantao Zuo:** Conceptualization, Funding acquisition, Supervision. **David Eidelberg:** Conceptualization, Supervision, Resources. **Jian Wang:** Conceptualization, Funding acquisition, Supervision, Project administration. **Yilong Ma:** Conceptualization, Methodology, Funding acquisition, Supervision, Writing - review & editing.

Declaration of Competing Interest

The authors declare that they have no known competing financial interests or personal relationships that could have appeared to influence the work reported in this paper.

Acknowledgments

The study at the Chinese site was funded jointly by the National Key R&D Program (2016YFC1306504) from the Ministry of Science and Technology of China, by the National Natural Science Foundation of China (91949118, 81771372, 81701250, 81361120393, and 81671239), Shanghai Municipal Science and Technology Major Project (No. 2017SHZDZX01, 2018SHZDZX03) and Science and Technology Commission of Shanghai Municipality (19441903500, 17JC1401600). The study at the American site was supported by the US-China Biomedical Collaborative Research Program (R01 NS083490) from the National Institutes of Health (NIH). The content is solely the responsibility of the authors and does not necessarily represent the official views of the NIH. The sponsors played no roles in study design; in the collection, analysis and interpretation of data; in the writing of the report; and in the decision to submit the article for publication.

Appendix A. Supplementary data

Supplementary data to this article can be found online at https://doi.org/10.1016/j.nicl.2020.102416.

References

Boxer, A.L., Yu, J.T., Golbe, L.I., Litvan, I., Lang, A.E., Höglinger, G.U., 2017. Advances in progressive supranuclear palsy: new diagnostic criteria, biomarkers, and therapeutic approaches. Lancet Neurol. 16, 552–563.

Caligiore, D., Pezzulo, G., Baldassarre, G., Bostan, A.C., Strick, P.L., Doya, K., Helmich, R.C., Dirkx, M., Houk, J., Jörntell, H., Lago-Rodriguez, A., Galea, J.M., Miall, R.C., Popa, T., Kishore, A., Verschure, P.F.M.J., Zucca, R., Herreros, I., 2017. Consensus Paper: Towards a Systems-Level View of Cerebellar Function: the Interplay Between Cerebellum, Basal Ganglia, and Cortex. Cerebellum 16, 203–229.

Chen, C.H., Fremont, R., Arteaga-Bracho, E.E., Khodakhah, K., 2014. Short latency cerebellar modulation of the basal ganglia. Nat. Neurosci. 17, 1767–1775.

Cummings, J.L., Henchcliffe, C., Schaier, S., Simuni, T., Waxman, A., Kemp, P., 2011. The role of dopaminergic imaging in patients with symptoms of dopaminergic system neurodegeneration. Brain 134, 3146–3166.

Eckert, T., Barnes, A., Dhawan, V., Frucht, S., Gordon, M.F., Feigin, A.S., Eidelberg, D., 2005. FDG PET in the differential diagnosis of parkinsonian disorders. Neuroimage 26, 912–921.

Eckert, T., Tang, C., Ma, Y., Brown, N., Lin, T., Frucht, S., Feigin, A., Eidelberg, D., 2008. Abnormal metabolic networks in atypical parkinsonism. Mov. Disord. 23, 727–733.

Federoff, M., Price, T.R., Sailer, A., Scholz, S., Hernandez, D., Nicolas, A., Singleton, A.B., Nalls, M., Houlden, H., 2016. Genome-wide estimate of the heritability of Multiple System Atrophy. Parkinsonism Relat. Disord. 22, 35–41.

Ge, J., Wu, J., Peng, S., Wu, P., Wang, J., Zhang, H., Guan, Y., Eidelberg, D., Zuo, C., Ma, Y., 2018. Reproducible network and regional topographies of abnormal glucose metabolism associated with progressive supranuclear palsy: Multivariate and univariate analyses in American and Chinese patient cohorts. Hum. Brain Mapp. 39, 2842–2858.

Gilman, S., Wenning, G.K., Low, P. a, Brooks, D.J., Mathias, C.J., Trojanowski, J.Q., Wood, N.W., Colosimo, C., Dürr, A., Fowler, C.J., Kaufmann, H., Klockgether, T., Lees, A.J., Poewe, W.H., Quinn, N.P., Revesz, T., Robertson, D., Sandroni, P., Seppi, K., Vidailhet, M., 2008. Second consensus statement on the diagnosis of multiple system atrophy. Neurology 71, 670–6.

Habeck, C., Foster, N.L., Perneczky, R., Kurz, A., Alexopoulos, P., Koeppe, R.A., Drzezga, A., Stern, Y., 2008. Multivariate and univariate neuroimaging biomarkers of Alzheimer's disease. Neuroimage 40, 1503–1515.

Hughes, A.J., Daniel, S.E., Ben-Shlomo, Y., Lees, A.J., 2002. The accuracy of diagnosis of parkinsonian syndromes in a specialist movement disorder service. Brain 125, 861–870.

Hughes, A.J., Daniel, S.E., Kilford, L., Lees, A.J., 1992. Accuracy of clinical diagnosis of idiopathic Parkinson's disease: a clinico-pathological study of 100 cases. J. Neurol. Neurosurg. Psychiatry 55, 181–184.

Jin, S., Oh, M., Oh, S.J., Oh, J.S., Lee, S.J., Chung, S.J., Kim, J.S., 2017. Additional Value

of Early-Phase 18F-FP-CIT PET Image for Differential Diagnosis of Atypical Parkinsonism. Clin. Nucl. Med. 42, e80–e87.
Kaasinen, V., Kankare, T., Joutsa, J., Vahlberg, T., 2019. Presynaptic striatal dopaminergic function in atypical parkinsonisms: A meta-analysis of imaging studies. J. Nucl. Med. 60, 1757–1763.
Ko, J.H., Lee, C.S., Eidelberg, D., 2017. Metabolic network expression in parkinsonism: Clinical and dopaminergic correlations. J. Cereb. Blood Flow Metab. 37, 683–693.
Kraemmer, J., Kovacs, G.G., Perju-Dumbrava, L., Pirker, S., Traub-Weidinger, T., Pirker, W., 2014. Correlation of striatal dopamine transporter imaging with post mortem substantia nigra cell counts. Mov. Disord. 29, 1767–1773.
Low, P.A., Reich, S.G., Jankovic, J., Shults, C.W., Stern, M.B., Novak, P., Tanner, C.M., Gilman, S., Marshall, F.J., Wooten, F., Racette, B., Chelimsky, T., Singer, W., Sletten, D.M., Sandroni, P., Mandrekar, J., 2015. Natural history of multiple system atrophy in the USA: A prospective cohort study. Lancet Neurol. 14, 710–719.
Lyoo, C.H., Jeong, Y., Ryu, Y.H., Lee, S.Y., Song, T.J., Lee, J.H., Rinne, J.O., Lee, M.S., 2008. Effects of disease duration on the clinical features and brain glucose metabolism in patients with mixed type multiple system atrophy. Brain 131, 438–446.
Ma, Y., Tang, C., Spetsieris, P.G., Dhawan, V., Eidelberg, D., 2007. Abnormal metabolic network activity in Parkinson's disease: test-retest reproducibility. J. Cereb. Blood Flow Metab. 27, 597–605.
Matthews, D.C., Lerman, H., Lukic, A., et al., 2018. FDG PET Parkinson's disease-related pattern as a biomarker for clinical trials in early stage disease. Neuroimage Clin. 20, 572–579.
Nemmi, F., Pavy-Le Traon, A., Phillips, O.R., et al., 2019. A totally data-driven whole-brain multimodal pipeline for the discrimination of Parkinson's disease, multiple system atrophy and healthy control. Neuroimage Clin. 23, 101858.
Obelieniene, D., Bauzaite, S., Kulakiene, I., Keleras, E., Eitmonaite, I., Rastenyte, D., 2018. Diagnostic challenges in multiple system atrophy. Neuropsychiatr. Dis. Treat. 14, 179–184.
Oh, M., Kim, J.S., Kim, J.Y., Shin, K.-H., Park, S.H., Kim, H.O., Moon, D.H., Oh, S.J., Chung, S.J., Lee, C.S., 2012. Subregional Patterns of Preferential Striatal Dopamine Transporter Loss Differ in Parkinson Disease, Progressive Supranuclear Palsy, and Multiple-System Atrophy. J. Nucl. Med. 53, 399–406.
Peng, S., Ma, Y., Spetsieris, P.G., Mattis, P., Feigin, A., Dhawan, V., Eidelberg, D., 2014. Characterization of disease-related covariance topographies with SSMPCA toolbox: effects of spatial normalization and PET scanners. Hum Brain Mapp 35, 1801–1814.
Poston, K.L., Tang, C.C., Eckert, T., Dhawan, V., Frucht, S., Vonsattel, J.-P., Fahn, S., Eidelberg, D., 2012. Network correlates of disease severity in multiple system atrophy. Neurology 78, 1237–1244.
Respondek, G., Roeber, S., Kretzschmar, H., Troakes, C., Al-Sarraj, S., Gelpi, E., Gaig, C., Chiu, W.Z., van Swieten, J.C., Oertel, W.H., Höglinger, G.U., 2013. Accuracy of the national institute for neurological disorders and stroke/society for progressive supranuclear palsy and neuroprotection and natural history in Parkinson plus syndromes criteria for the diagnosis of progressive supranuclear palsy. Mov. Disord. 28, 504–509.
Rizzo, G., Copetti, M., Arcuti, S., Martino, D., Fontana, A., Logroscino, G., 2016. Accuracy of clinical diagnosis of Parkinson disease. Neurology 86, 566–576.
Schindlbeck, K.A., Eidelberg, D., 2018. Network imaging biomarkers: insights and clinical applications in Parkinson's disease. Lancet Neurol. 17, 629–640.
Spetsieris, P.G., Ma, Y., Dhawan, V., Eidelberg, D., 2009. Differential diagnosis of parkinsonian syndromes using PCA-based functional imaging features. Neuroimage 45, 1241–1252.
Stamelou, M., Bhatia, K.P., 2016. Atypical parkinsonism - New advances. Curr. Opin. Neurol. 29, 480–485.
Stoessl, A.J., Lehericy, S., Strafella, A.P., Shulman, G., 2014. Imaging insights into basal ganglia function, Parkinson's disease, and dystonia. Lancet 384, 532–544.
Südmeyer, M., Antke, C., Zizek, T., Beu, M., Nikolaus, S., Wojtecki, L., Schnitzler, A., Müller, H.-W.W., 2011. Diagnostic accuracy of combined FP-CIT, IBZM, and MIBG scintigraphy in the differential diagnosis of degenerative parkinsonism: A multidimensional statistical approach. J. Nucl. Med. 52, 733–740.
Tang, C.C., Poston, K.L., Eckert, T., Feigin, A., Frucht, S., Gudesblatt, M., Dhawan, V., Lesser, M., Vonsattel, J.P., Fahn, S., Eidelberg, D., 2010. Differential diagnosis of parkinsonism: a metabolic imaging study using pattern analysis. Lancet Neurol. 9, 149–158.
Tatsch, K., Poepperl, G., 2013. Nigrostriatal Dopamine Terminal Imaging with Dopamine Transporter SPECT: An Update. J. Nucl. Med. 54, 1331–1338.
Teune, L.K., Bartels, A.L., De Jong, B.M., Willemsen, A.T.M., Eshuis, S.A., De Vries, J.J., Van Oostrom, J.C.H., Leenders, K.L., 2010. Typical cerebral metabolic patterns in neurodegenerative brain diseases. Mov. Disord. 25, 2395–2404.
Teune, L.K., Renken, R.J., Mudali, D., De Jong, B.M., Dierckx, R.A., Roerdink, J.B.T.M., Leenders, K.L., 2013. Validation of parkinsonian disease-related metabolic brain patterns. Mov. Disord. 28, 547–551.
Tong, J., Wong, H., Guttman, M., Ang, L.C., Forno, L.S., Shimadzu, M., Rajput, A.H., Muenter, M.D., Kish, S.J., Hornykiewicz, O., Furukawa, Y., 2010. Brain α-synuclein accumulation in multiple system atrophy, Parkinson's disease and progressive supranuclear palsy: A comparative investigation. Brain 133, 172–188.
Tripathi, M., Tang, C.C., Feigin, A., De Lucia, I., Nazem, A., Dhawan, V., Eidelberg, D., 2016. Automated Differential Diagnosis of Early Parkinsonism Using Metabolic Brain Networks: A Validation Study. J. Nucl. Med. 57, 60–66.
Van Laere, K., Santens, P., Bosman, T., De Reuck, J., Mortelmans, L., Dierckx, R., 2004. Statistical parametric mapping of 99mTc-ECD SPECT in idiopathic Parkinson's disease and multiple system atrophy with predominant parkinsonian features: Correlation with clinical parameters. J. Nucl. Med. 45, 933–942.
Van Laere, K., Clerinx, K., D'Hondt, E., de Groot, T., Vandenberghe, W., 2010. Combined Striatal Binding and Cerebral Influx Analysis of Dynamic 11C-Raclopride PET Improves Early Differentiation Between Multiple-System Atrophy and Parkinson Disease. J. Nucl. Med. 51, 588–595.
Wu, P., Wang, J., Peng, S., Ma, Y., Zhang, H., Guan, Y., Zuo, C., 2013. Metabolic brain network in the Chinese patients with Parkinson's disease based on18F-FDG PET imaging. Park. Relat. Disord. 19, 622–627.
Yang, H., Wang, N., Luo, X., et al., 2019. Cerebellar atrophy and its contribution to motor and cognitive performance in multiple system atrophy. Neuroimage Clin. 23, 101891.